MONITORING FATIGUE DAMAGE IN CFRP USING ULTRASONIC BIREFRINGENCE

Peter Fey[1] and Marc Kreutzbruck[2]

[1]Institut für Kunststofftechnik, University of Stuttgart, Germany
Email: Peter.Fey@ikt.uni-stuttgart.de, Web Page: http://www. ikt.uni-stuttgart.de
[2] Institut für Kunststofftechnik, University of Stuttgart, Germany
Email: Marc.Kreutzbruck @ikt.uni-stuttgart.de, Web Page: http://www. ikt.uni-stuttgart.de

Keywords: fatigue, non-destructive testing, ultrasound, anisotropy, CFRP

Abstract

Fiber reinforced plastics (FRP) are in widespread use for high performance applications such as aerospace, wind energy, and automotive as well as leisure and sports articles. If lightweight structures are needed, engineers prefer them over metals due to their superior weight to stiffness ratio. By constructing laminates with different fiber directions, the material can be tailored to the load case. Unlike metals, which show rust or dents, FRP do not allow their degradation to be easily detected by visual testing. Degradation of FRP under cyclic loading occurs in the form of microscopic matrix cracks. These occur first where the fibers are not aligned to the loading direction. When increasing the number of load cycles one also observes an increase in crack density. From areas of high crack density the cracks spread throughout the whole material until final failure. Because many of the aforementioned applications imply long term usage and a high risk to the user if the structure fails, testing methods for integrity assessment are needed.

The high elastic anisotropy in FRP is a great challenge for non-destructive testing methods. But it also opens the opportunity for specialized methods like ultrasonic birefringence, which is able to exploit the anisotropy for material damage state characterization. Ultrasonic birefringence is based on the difference between propagation velocity of transverse ultrasonic waves polarized parallel respectively perpendicular to the fiber direction when propagating in through thickness direction. This velocity difference characterizes the integrity of a single ply. Interference effects occur at the interfaces between plies, too. Both effects can be modelled using a physics based model. Using the model and comparing modelled and measured results, the evolution of fatigue damage in quasi-isotropic CFRP specimen subjected to cyclic loading was monitored and damage was characterized for each fiber direction in the layup.

1. Introduction

In the face of new technological challenges to yield even better CO2 emission reduction, lightweight construction is reaching out from high performance applications like aerospace industry, sports cars, or wind energy to more mass production areas such as road vehicles like the BMW i3. Fiber reinforced plastics (FRP) are used in many of these applications because of their superior stiffness-to-weight and strength-to-weight ratios. The combination of fibers and polymer matrix also allows for much greater flexibility in the shapes of structures as well as integration of functionality. Also they are more robust against environmental influences like oxidation.

Excerpt from ISBN 978-3-00-053387-7

The mix of high strength and high stiffness fibers with low strength and low stiffness matrix makes the damage mechanisms in FRP complex. A standard way of using FRP is layups, by which plies of FRP with different fiber orientations are stacked on top of each other. The fiber orientations are chosen depending on the direction of the expected loads. Because of that, in almost every FRP-part plies exist whose fibers are not aligned parallel to the load that is applied to it. In these plies, fatigue damage is initiated by formation of so called transverse cracks, which are parallel to the fibers but perpendicular to the plane of the plies and extend through the entire thickness of the plies [1–8]. Most of these cracks form in the beginning of fatigue life, until a saturation level is reached. The transverse crack growth rates depend on thickness, orientation and stacking sequence of the plies [1, 4, 5, 8]. They do promote the formation of delaminations between the plies because stress concentrations arise at their tips [3], also leading to fiber fracture which usually equals ultimate failure of the laminate [4].

The stiffness decay due to these cracks has been detected using ultrasound in an immersion bath to measure the bulk velocities [9] or lamb wave velocities exited using contact [10] and air-coupled [11] ultrasound transducers. These methods all yield information about the overall state of a laminate. Another method, ultrasonic birefringence, was first applied to the problem of fatigue of FRP in [12], and will be presented here.

The term birefringence describes the phenomenon of polarization direction dependent propagation velocity of waves. It is textbook knowledge in optics [13] and also exists for ultrasound. Applications of the ultrasonic version are in-situ detection of polymer molecule orientation in semi-crystalline polymers during injection molding [14], detection of layup errors in the production of composite parts [15], characterization of texture in rolled metals [16] or more academic rotation of the polarization direction of a shear wave by using CFRP with a chiral layup sequence [17].

2. Materials and Methods

2.1 Birefringence Measurement Setup

The setup for birefringence measurements of [12] consists of a shear wave transducer (Krautkrämer K4KY) which is rotated by a stepper motor in 3.6° steps (Figure. 1). The couplant was SLC 70, GE Inspection Technologies, Hürth, Germany. At each step an a-scan is made by the Ritec SNAP RAM-5000 ultrasound system, which uses its heterodyne receiver unit to detect amplitude and phase of the back wall echo. Amplitude and phase are then plotted over the transducer rotation angle to yield the curves presented in the results section. Measurements were performed on five locations of the specimens and then averaged.

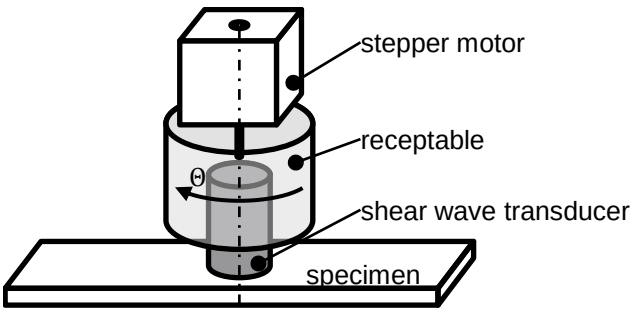

Figure. 1. Schematic setup for birefringence measurements

2.2 CFRP Fatigue

The specimens of [12] were 25 mm wide and 250 mm long CFRP-strips with a thickness of 3.1 mm made from Hexcel HexPly® M18/1 UD G947. GFRP/aluminum end tabs were used, fatiguing was performed in an Instron 8502 servo hydraulic testing machine at 80% static tensile failure load. Cyclic

Excerpt from ISBN 978-3-00-053387-7

loading was interrupted at predefined numbers of cycles to perform the ultrasonic birefringence measurements.

3. Theory

To model birefringence in layered composites, multiple theories have been developed. One theory, which is used in e. g. [18, 19] and traces back to the works of Thomson [20] and Haskell [21], calculates effective reflection and transmission coefficients for ultrasonic waves of arbitrary polarization and incidence angle on the laminate even accounting for longitudinal-transverse mode conversions. It does not include attenuation, but accounts for all reflections between the plies. To perform the calculation using that model, all stiffnesses of the material need to be known.

Another model is the ply-by-ply vector decomposition model presented in [15]. Its basic assumption is that the shear wave, which is incident perfectly perpendicular on the specimens surface, splits in two parts being polarized parallel and perpendicular to the fibers. At an interface between two plies whose fibers are not aligned parallel to each other, each of the two waves splits up again in two parts, one parallel and one perpendicular to the fibers in the second ply, yielding four waves. Since this happens at each interface, for N plies 2^N waves will be arriving at the opposite end of the ply. The splitting is calculated by projecting the waves polarisation direction onto the fiber direction. The velocity difference between the polarisation directions is included in the model via time shifts of the waves according to thickness and phase velocity in the plies. The waves are represented by digitized a-scans, which were shifted in time and multiplied by factors calculated from the splitting operations. Hence for N plies in a transmission setup 2^N digitized a-scans had to be processed and summed up. Even though simplifications for plies of equal fiber direction are possible, the computational expense is high. This model may be calculated using only the shear stiffnesses for polarization parallel and perpendicular to the fibers, but also includes attenuation.

In [12] a model is presented which uses the same mechanism for representation of the wave splitting at interfaces between the plies as the previous one. But instead of using digitized a-scans to represent the ultrasonic waves, each wave is represented as a complex number with its amplitude being the magnitude and phase information encapsulated in the argument. Also the number of waves does not increase because at each interface between two plies the waves from the previous ply are recombined. This reduces the computational expense to only a few matrix multiplications and hence made extensive parameter variations in a short time feasible.

For the sake of simplicity, the model is limited to waves traversing the plies perpendicular to their plane. It is based on two basic effects:

- Phase shift and attenuation within the plies
- Interference of the incident waves and decomposition into partial waves at the interfaces

Phase shift and attenuation of a wave with polarization direction parallel (∥) propagating in ply n of a layup can be described by

$$P_{n\parallel} = exp(-\alpha_{n\parallel} d_n)\, exp\left(-j\omega d_n \sqrt{\frac{\rho_n}{G_{n\parallel}}}\right)$$

with angular frequency ω, thickness d_n, density ρ_n, attenuation constant α_n and shear modulus G_n. Obviously the same is valid if the wave was polarized perpendicular to the fibers, in the model only the index would have to be changed to $\perp$. Both waves, polarized parallel and perpendicular to the fibers, are combined in a matrix

Excerpt from ISBN 978-3-00-053387-7

$$\bar{\bar{P}}_n = \begin{pmatrix} P_{n\parallel} & 0 \\ 0 & P_{n\perp} \end{pmatrix}$$

to represent ply n.

The interface between two plies n and m is represented by a simple coordinate transform in matrix form

$$\bar{\bar{I}}_{n,m} = \begin{pmatrix} cos\,\Delta\theta_{n,m} & sin\,\Delta\theta_{n,m} \\ -sin\,\Delta\theta_{n,m} & cos\,\Delta\theta_{n,m} \end{pmatrix},$$

just as it would be used to transform points between two coordinate systems of which one has been rotated about the origin by an angle $\Delta\theta_{n,m}$, which is the difference between the fiber orientation angles in the two plies. The two types of matrices are the used to represent the laminate by just multiplying them together from right to left. A 0°/90° layup in a transmission setup would hence be represented by

$$\bar{\bar{L}}_{[(0°/90°)transmission]} = \bar{\bar{P}}_{90°}\bar{\bar{I}}_{0°,90°}\bar{\bar{P}}_{0°}.$$

In this case, as will be done in the rest of the paper, the index n indicates the fiber direction in the ply. If the measurement was instead performed in reflection mode, also the wave traversing back from the back wall to the transducer would have to be included in the model, yielding

$$\bar{\bar{L}}_{[(0°/90°)reflection]} = \bar{\bar{P}}_{0°}\bar{\bar{I}}_{90°,0°}\bar{\bar{P}}_{90°}\bar{\bar{P}}_{90°}\bar{\bar{I}}_{0°,90°}\bar{\bar{P}}_{0°}.$$

In this case it should be noted that not only the order in which the matrices are multiplied is important, but also the direction of an interface matrix matters, because generally $\bar{\bar{I}}_{n,m} \neq \bar{\bar{I}}_{m,n}$.

The link between the theory and real measurements is closed by including a vector $\bar{A}_{in}$ of incident amplitude and a vector $\bar{A}_{out}$ of received amplitude. The first component of these vectors is the amplitude parallel to the transducers polarization direction, the second one is the amplitude polarized perpendicular to it, which is not detectable. To account for the orientation Θ of the transducer, also interface matrices for the interface between transducer and laminate need to be included.

$$\bar{A}_{out} = \begin{pmatrix} \bar{A}_{\parallel out} \\ \bar{A}_{\perp out} \end{pmatrix} = \bar{\bar{I}}_{0°,\Theta}\bar{\bar{L}}_{[(0°/90°)\text{reflection}]}\bar{\bar{I}}_{\Theta,0°}\begin{pmatrix} A_{\parallel in} \\ 0 \end{pmatrix}$$

4. Results and Discussion

To match measured values with modelled values, values measured were displayed as individual phase and amplitude curves. To cope with measurement uncertainties due to unequal couplant layer thickness, phase values were shifted such that their minima were aligned and amplitude curves were scaled to a maximum of one. Input parameters to the model were varied until measured and simulated curves were visually matching each other. The parameters varied were the shear stiffnesses perpendicular to the fibers $G_\perp$ in the 90°-, 45°-, and 45°-plies as well as the correspondig attenuations. 0°-ply properties as well as stiffnesses and attenuations for waves polarized parallel to the fibers were not varied, which is in accordance with the findings on FRP fatigue listed in the introduction. The measured and simulated curves are displayed in Fig. 2, while the stiffnesses and attenuations used in the simulations are given in Fig. 3.

An increase in the difference between maximum and minimum phase is seen during the fatigue life, which can be partially attributed to damage in the 90°-plies. But also a shift of the amplitude curves maximum from about 90° transducer orientation to approximately 120° indicates that damage must progress stronger in the -45° plies than in the +45°-plies. A saw tooth to rectangular shape deformation

Excerpt from ISBN 978-3-00-053387-7

of the phase curve is seen in the measured phase curves, which is attributed to attenuation increase in the -45° plies. Attentive readers will notice that one simulated curve seems to be missing. This is due to almost complete coincidence of two successive measurement results.

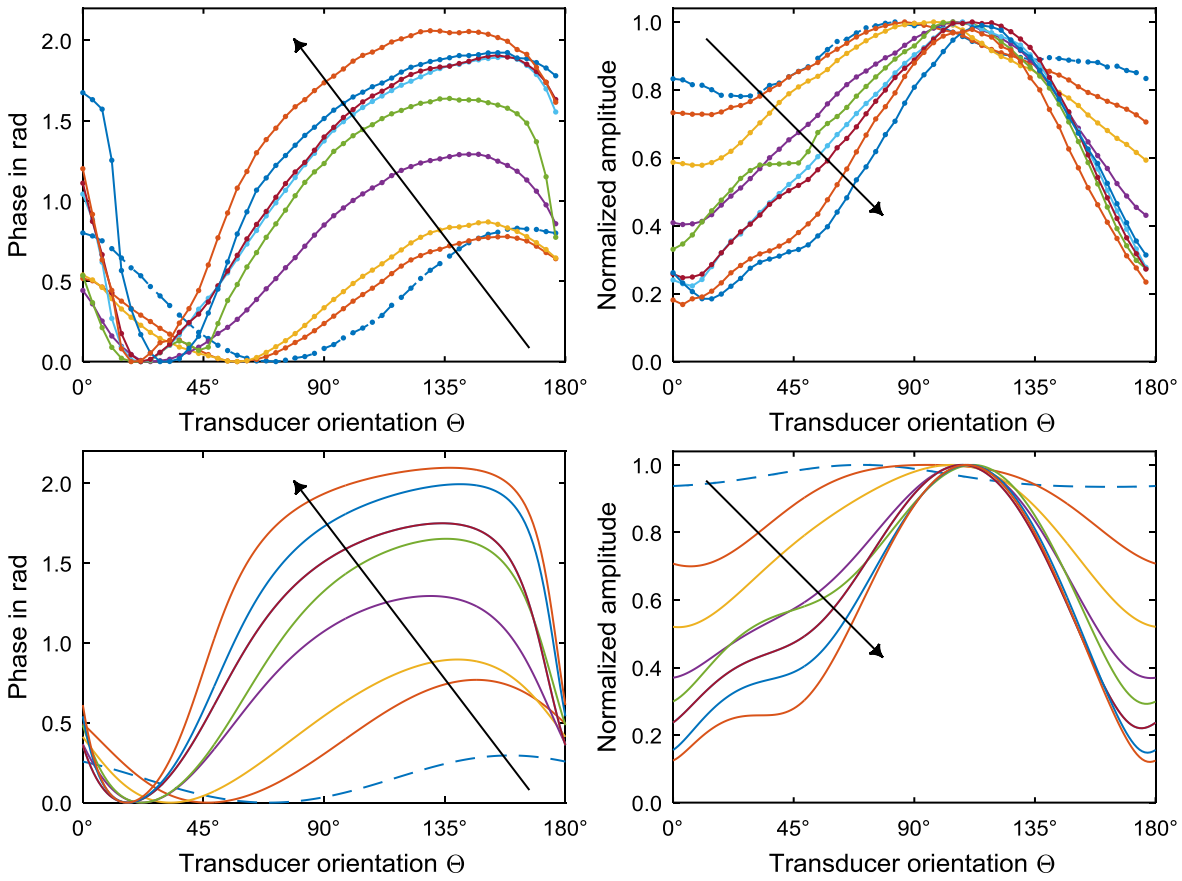

Fig. 2. Measured (top) and simulated (bottom) phase (left) and amplitude (right) curves of fatigue tracking measurement. Simulated curves were generated using values from Fig. 3. Arrows indicate increasing number of fatigue cycles.

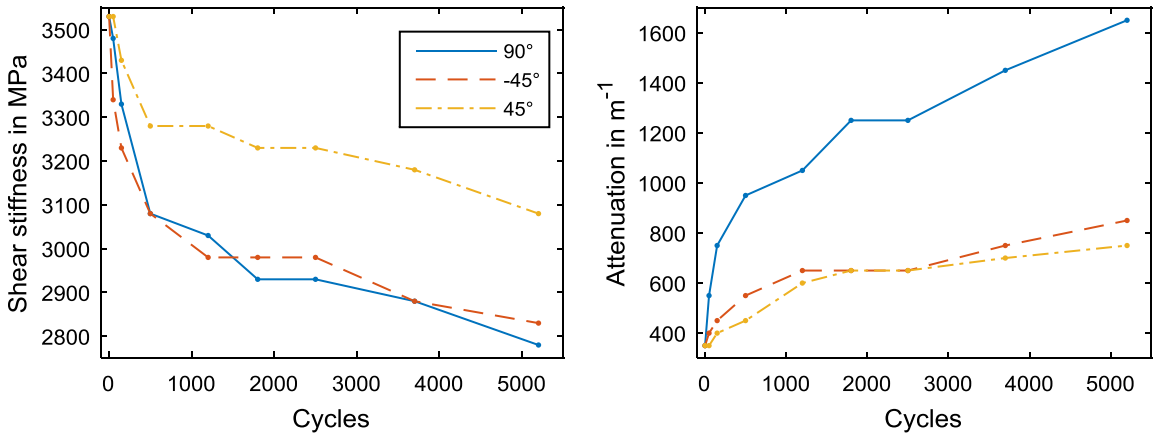

Fig. 3. Material properties used to generate the curves in the bottom row of Fig. 2

The shear stiffnesses and attenuations obtained by the matching of measured curves with simulations (Fig. 3) do reflect the damage progression anticipated from the literature very well. Especially the

Excerpt from ISBN 978-3-00-053387-7

rapid decrease in the beginning of fatigue life is reflected. The reason for larger stiffness decrease in the -45°-plies as compared to the 45°-plies is to be found in the nature of the layup. In the [0°/45°/90°/-45°]S2 layup the -45°-plies are twice as thick as the others (because [A/B]S = [A/B/B/A]) and they are located between 90°-plies. Both facts are reasons for accelerated damage progression in these plies, since thicker plies are more susceptible to damage and crack in the 90° plies induce stress concentrations in the neigboring plies. However it is unclear as to why the attenuations of the 45°- and -45°-plies appear to remain almost equal.

5. Summary

Ultrasonic birefringence was used to track the evolution of fatigue damage in CFRP under cyclic tensile load. Shear stiffnesses and attenuations could be obtained by matching of measured and modelled data. Besides the simplicity of the measurement setup the possibility to extract fiber direction resolved information makes it more detailed than methods which only give general information about FRP damage state.

The potential of the method should be further extended by inclusion of reflections (like in [18]), but also attenuation (as presented in [12] and [15]), scattering, and finite length pulses (as in [15]). Accounting for these effects should enable the method to also differentiate between damage in different depths in the specimens as well as give further information about the kind of damage from scattering.

References

[1] CROSSMAN, F.W. and A.S.D. WANG. The dependence of transverse cracking and delamination on ply thickness in graphite/epoxy laminates. In: K.L. REIFSNIDER, Hg. *Damage in composite materials, ASTM STP 775:* American Society for Testing and Materials, 1982, S. S. 118-139.

[2] CHAREWICZ, A. and I.M. DANIEL. Damage mechanisms and accumulation in graphite/epoxy laminates. In: H.T. HAHN, Hg. *Composite Materials: Fatigue and Fracture, ASTM STP 907.* Philadelphia, 1986, S. S. 274-297. ISBN 978-0-8031-0470-9.

[3] NAIRN, J.A. and S. HU. The initiation and growth of delaminations induced by matrix microcracks in laminated composites. In: *International Journal of Fracture,* 1992, **57**, S. 1-24. Doi:10.1007/BF00013005

[4] TONG, J. Characteristics of fatigue crack growth in GFRP laminates. In: *International Journal of Fatigue,* 2002, **24**, S. 291-297. Doi:10.1016/S0142-1123(01)00084-6

[5] YOKOZEKI, T., T. AOKI, T. OGASAWARA and T. ISHIKAWA. Effects of layup angle and ply thickness on matrix crack interaction in contiguous plies of composite laminates. In: *Composites Part A,* 2005, **36**(9), S. 1229-1235. Doi:10.1016/j.compositesa.2005.02.002

[6] ADDEN, S. and P. HORST. Stiffness degradation under fatigue in multiaxially loaded non-crimped-fabrics. In: *International Journal of Fatigue,* 2010, **32**(1), S. 108-122. Doi:10.1016/j.ijfatigue.2009.02.002

[7] GAGEL, A., D. LANGE and K. SCHULTE. On the relation between crack densities, stiffness degradation, and surface temperature distribution of tensile fatigue loaded glass-fibre non-crimp-fabric reinforced epoxy. In: *Composites Part A,* 2006, **37**(2), S. 222-228. Doi:10.1016/j.compositesa.2005.03.028

Excerpt from ISBN 978-3-00-053387-7

[8] REIFSNIDER, K. Fatigue behavior of composite materials. In: *International Journal of Fracture*, 1980, **16**(6), S. 563-583. http://www.springerlink.com/index/M401Q5085314R7N8.pdf

[9] BÖHM, R. and W. HUFENBACH. Experimentally based strategy for damage analysis of textile-reinforced composites under static loading. In: *Composites Science and Technology*, 2010, **70**(9), S. 1330-1337. Doi:10.1016/j.compscitech.2010.04.008

[10] SEALE, M.D., B.T. SMITH and W.H. PROSSER. Lamb wave assessment of fatigue and thermal damage in composites. In: *The Journal of the Acoustical Society of America*, 1998, **103**(5), S. 2416-2424. http://scholar.google.com/scholar?hl=en&btnG=Search&q=intitle:Lamb+wave+assessment+of+fatigue+and+thermal+damage+in+composites#0

[11] RHEINFURTH, M., N. KOSMANN, D. SAUER, G. BUSSE and K. SCHULTE. Lamb waves for non-contact fatigue state evaluation of composites under various mechanical loading conditions. In: *Composites Part A*, 2012, **43**(8), S. 1203-1211. Doi:10.1016/j.compositesa.2012.03.021

[12] RHEINFURTH, M., P. FEY, S. ALLINGER and G. BUSSE. Ultrasonic birefringence as a measure of mechanically induced fatigue damage in laminated composites. In: *International Journal of Fatigue*, 2013, **48**, S. 80-89. Doi:10.1016/j.ijfatigue.2012.10.005

[13] HECHT, E. *Optik.* 3., vollst. überarb. Aufl. München: Oldenbourg, 2001. ISBN 3-486-24917-7.

[14] EDWARDS, R. and C. THOMAS. Online measurement of polymer orientation using ultrasonic technology. In: *Polymer Engineering & Science*, 2001, **41**(9).

[15] FISCHER, B.A. and D.K. HSU. Application of shear waves for composite laminate characterization. In: *Review of Progress in Quantitative Nondestructive Evaluation*, 1996, **15**, S. 1191-1198. http://scholar.google.com/scholar?hl=en&btnG=Search&q=intitle:Application+of+shear+waves+for+composite+laminate+characterization#0

[16] SCHNEIDER, E. Ultrasonic birefringence effect–Its application for materials characterisations. In: *Optics and Lasers in Engineering*, 1995, **22**(4-5), S. 305-323. http://www.sciencedirect.com/science/article/pii/0143816694000326

[17] VARADAN, V.V., S.K. YANG and V.K. VARADAN. Rotation of Elastic Shear Waves in Laminated , Structurally Chiral Composites. In: *Journal of Sound and Vibration*, 1992, **159**(3), S. 403-420.

[18] YANG, S.-K., V.V. VARADAN, A. LAKHTAKIA and V.K. VARADAN. Reflection and transmission of elastic waves by a structurally chiral arrangement of identical uniaxial layers. In: *Journal of Physics D: Applied Physics*, 1991, **24**, S. 1601-1608. http://iopscience.iop.org/0022-3727/24/9/012

[19] ROKHLIN, S.I. and L. WANG. Stable recursive algorithm for elastic wave propagation in layered anisotropic media: Stiffness matrix method. In: *The Journal of the Acoustical Society of America*, 2002, **112**(3), S. 822. Doi:10.1121/1.1497365

[20] THOMSON, W.T. Transmission of Elastic Waves through a Stratified Solid Medium. In: *Journal of Applied Physics*, 1950, **21**(2), S. 89. Doi:10.1063/1.1699629

[21] HASKELL, N.A. The dispersion of surface waves on multilayered media. In: *Bulletin of the Seismological Society of America*, 1953, **43**(1), S. 17-34.